AFRL-PR-WP-TP-2005-208

A LARGE-SCALE INVESTIGATION OF A FLAT-PLATE PULSED VORTEX GENERATOR JET IN CROSSFLOW USING PIV

Marc Polanka and Rolf Sondergaard (AFRL/PRTT)

Kenneth Moore and Mitch Wolff (Wright State University)

July 2005

Approved for public release; distribution is unlimited.

STINFO FINAL REPORT

PROPULSION DIRECTORATE
AIR FORCE RESEARCH LABORATORY
AIR FORCE MATERIEL COMMAND
WRIGHT-PATTERSON AIR FORCE BASE, OH 45433-7251

NOTICE

Using Government drawings, specifications, or other data included in this document for any purpose other than Government procurement does not in any way obligate the U.S. Government. The fact that the Government formulated or supplied the drawings, specifications, or other data does not license the holder or any other person or corporation; or convey any rights or permission to manufacture, use, or sell any patented invention that may relate to them.

This report was cleared for public release by the Air Force Research Laboratory Wright Site Public Affairs Office (AFRL/WS) and is releasable to the National Technical Information Service (NTIS). It will be available to the general public, including foreign nationals.

Public Affairs case number: AFRL-WS-05-1191
Date cleared: 17-May-2005

THIS TECHNICAL REPORT IS APPROVED FOR PUBLICATION.

_____//s//_____
ROLF SONDERGAARD, Ph.D.
Project Monitor
Turbine Branch

_____//s//_____
CHARLES W. STEVENS
Chief
Turbine Branch

_____//s//_____
WILLIAM W. COPENHAVER, Ph.D.
Principal Scientist
Turbine Engine Division

This report is published in the interest of scientific and technical information exchange and its publication does not constitute approval or disapproval of its ideas or findings.

REPORT DOCUMENTATION PAGE

Form Approved
OMB No. 0704-0188

1. REPORT DATE *(DD-MM-YY)*	2. REPORT TYPE	3. DATES COVERED *(From - To)*
July 2005	Conference paper postprint	07/10/05 – 07/13/05

4. TITLE AND SUBTITLE
A LARGE-SCALE INVESTIGATION OF A FLAT-PLATE PULSED VORTEX GENERATOR JET IN CROSSFLOW USING PIV

5a. CONTRACT NUMBER
In-House

5b. GRANT NUMBER

5c. PROGRAM ELEMENT NUMBER
61102F

6. AUTHOR(S)
Marc Polanka and Rolf Sondergaard (AFRL/PRTT)

Kenneth Moore and Mitch Wolff (Wright State University)

5d. PROJECT NUMBER
2307

5e. TASK NUMBER
NP

5f. WORK UNIT NUMBER
2307NP02

7. PERFORMING ORGANIZATION NAME(S) AND ADDRESS(ES)

Turbine Branch (PRTC)
Turbine Engine Division
Propulsion Directorate
Air Force Materiel Command, Air Force Research Laboratory
Wright-Patterson AFB, OH 45433-7251

Wright State University

8. PERFORMING ORGANIZATION REPORT NUMBER
AFRL-PR-WP-TP-2005-208

9. SPONSORING/MONITORING AGENCY NAME(S) AND ADDRESS(ES)

Propulsion Directorate
Air Force Research Laboratory
Air Force Materiel Command
Wright-Patterson AFB, OH 45433-7251

10. SPONSORING/MONITORING AGENCY ACRONYM(S)
AFRL/PRTT

11. SPONSORING/MONITORING AGENCY REPORT NUMBER(S)
AFRL-PR-WP-TP-2005-208

12. DISTRIBUTION/AVAILABILITY STATEMENT
Approved for public release; distribution is unlimited.

13. SUPPLEMENTARY NOTES
Presented at the 41st AIAA/ASME/SAE/ASEE Joint Propulsion Conference and Exhibit, Tucson, AZ, 10-13 July 2005. This material is declared a work of the U.S. Government and is not subject to copyright protection in the United States.

14. ABSTRACT
The use of small jets of air has proved to be an effective means of flow control on low Reynolds number turbine blades. Pulsing of these jets has also shown benefits in reducing the amount of air needed to achieve the same level of flow control. An experiment using Particle Image Velocimetry (PIV) has been set up to investigate how these pulsed jets interact with the boundary layer to help stabilize it and keep the flow attached. A 25x scaled jet in a plate has been utilized. The 25.4 mm diameter jet has a pitch angle of 30° and a skew angle of 90°. Pitch angle is defined as the angle the jet makes with the surface of the plate, and the skew angle is the angle that the jet makes with the cross flow. The jet was pulsed at a frequency of f = 0.5 Hz with duty cycle (pulse duration of the total period T) of $\Delta = 50\%$.
Blowing ratios $\rho_j V_j/\rho_\infty U_\infty$, or ratios of jet velocity, V_j, to freestream velocity, U_∞, when the densities ρ_j and ρ_∞ are equal) of B = 0, 0.5, 1, 2, and 4 were studied. A reduced frequency parameter was defined as $F^+ = fl/U_\infty$, with the reference length l equal to the jet diameter, d, resulting in $F^+ = 0.004$ with $U_\infty = 3.15$ m/s. Velocity and vorticity planes were obtained at different spanwise locations and used in the characterization of the flow. Based on previous research, the starting vortex, which develops at the beginning of every cycle for each pulsed case, is the critical flow characteristic. The current study shows that both the starting and ending of every duty cycle are keys to obtaining attached flow, and that attachment is improved with larger in-plane vorticity, ω_j.

15. SUBJECT TERMS

16. SECURITY CLASSIFICATION OF:			17. LIMITATION OF ABSTRACT:	18. NUMBER OF PAGES	19a. NAME OF RESPONSIBLE PERSON (Monitor)
a. REPORT	b. ABSTRACT	c. THIS PAGE			Rolf Sondergaard
Unclassified	Unclassified	Unclassified	SAR	16	19b. TELEPHONE NUMBER *(Include Area Code)* (937) 255-7190

Standard Form 298 (Rev. 8-98)
Prescribed by ANSI Std. Z39-18

41st AIAA/ASME/SAE/ASEE Joint Propulsion
Conference and Exhibit, Tucson, Arizona
10–13 July 2005

AIAA-2005-4221

A Large-Scale Investigation of a Flat-Plate Pulsed Vortex Generator Jet in Crossflow Using PIV

Kenneth Moore* and Mitch Wolff†
Wright State University, Dayton, Ohio, 45435

Marc Polanka‡ and Rolf Sondergaard§
Air Force Research Laboratory, WPAFB, Ohio, 45433

The use of small jets of air has proved to be an effective means of flow control on low Reynolds number turbine blades. Pulsing of these jets has also shown benefits in reducing the amount of air needed to achieve the same level of flow control. An experiment using Particle Image Velocimetry (PIV) has been set up to investigate how these pulsed jets interact with the boundary layer to help stabilize it and keep the flow attached. A 25x scaled jet in a plate has been utilized. The 25.4 mm diameter jet has a pitch angle of 30° and a skew angle of 90°. Pitch angle is defined as the angle the jet makes with the surface of the plate, and the skew angle is the angle that the jet makes with the cross flow. The jet was pulsed at a frequency of f = 0.5 Hz with duty cycle (pulse duration of the total period T) of Δ = 50%. Blowing ratios ($\rho_j V_j / \rho_\infty U_\infty$, or ratios of jet velocity, V_j, to freestream velocity, U_∞, when the densities ρ_j and ρ_∞ are equal) of B = 0, 0.5, 1, 2, and 4 were studied. A reduced frequency parameter was defined as $F^+ = f\,l\,/\,U_\infty$, with the reference length l equal to the jet diameter, d, resulting in F^+ = 0.004 with U_∞ = 3.15 m/s. Velocity and vorticity planes were obtained at different spanwise locations and used in the characterization of the flow. Based on previous research, the starting vortex, which develops at the beginning of every cycle for each pulsed case, is the critical flow characteristic. The current study shows that both the starting and ending of every duty cycle are keys to obtaining attached flow, and that attachment is improved with larger in-plane vorticity, ω_j.

Nomenclature

d	=	jet diameter
U_∞	=	freestream velocity
V_j	=	jet velocity
B	=	blowing ratio, $\rho_j V_j / \rho_\infty U_\infty$
Δ	=	duty cycle
l	=	reference length
f	=	pulsing frequency
T	=	cycle period, $1/f$
F^+	=	dimensionless forcing frequency, $f\,l\,/\,U_\infty$
ω_j	=	in-plane vorticity, normalized by U_∞/d
t	=	time, normalized by T
x, y, z	=	Cartesian coordinates used to define position

---

* Graduate Research Assistant, Department of Mechanical and Materials Engineering, 3640 Colonel Glenn Hwy, AIAA Student Member.

† Professor, Department of Mechanical and Materials Engineering, 3640 Colonel Glenn Hwy, AIAA Associate Fellow.

‡ Turbine Research Engineer, Propulsion Directorate, 1950 Fifth St.

§ Aerospace Engineer, Propulsion Directorate, 1950 Fifth St, AIAA member.

I. Introduction

Due to lower density air at high altitudes, the Reynolds number decreases and significant aerodynamic losses can occur in gas turbine engines. In the low pressure turbine, these losses are caused by flow separation near the trailing edge of the blade suction surface. Associated with the loss increase is a performance and efficiency decrease for the engine. By delaying flow separation, engine efficiency can be maintained at higher altitudes. These performance issues have prompted many attempts at controlling boundary layer separation.

Flow control techniques studied at the Air Force Research Laboratory (AFRL) include the use of dimples, plasma excitation, and vortex generator jets (VGJs). Lake[1] was able to improve the loss coefficient by over 50% by applying dimples at 65% axial chord on a Pak-B blade geometry in the Low Speed Wind Tunnel (LSWT) facility. Current work is being done using plasma flow,[2] while List, et al.,[3] have seen a reduction in loss coefficient of 14% at the Air Force Academy wind tunnel cascade (Langston blade geometry) using a plasma actuator. VGJs have long been studied as a flow separation technique on airfoils, but recent studies by Bons, et al.[4,5] in the LSWT have applied this technique to low pressure turbine (LPT) blades. They successfully found delayed flow separation on low Reynolds number turbine blades, reducing the loss coefficient by over 50%. In the Bons studies, pulsing the jets also proved to be effective, achieving the same benefits with up to an order of magnitude less mass flow.

The reasons for the separation delay and why pulsed jets are just as effective as steady jets are relatively unknown. Johari and McManus[6] performed a flat plate pulsed VGJ experiment in a water tunnel and found that the starting vortex is the cause of the improvement of pulsed VGJs over steady VGJs. Compton and Johnston[7] found that separation control benefits only occur if VGJs are pitched and skewed with the main flow direction, and that larger skew angles of 45 to 90 degrees produce the strongest vorticies. McManus et al. [8] found increased benefits at larger velocity ratios (blowing ratios). There are many variables that can factor into achieving the benefits of pulsed VGJs, and the mechanisms responsible for these benefits are not well understood. It is thus desirable to perform a detailed study of the flow physics of a pulsed VGJ and to visualize jet interaction with the boundary layer. A large scale flat plate model allows such a study.

The flat plate jet in this study is meant to be a large scale version of the jets on the Pack-B blade in the LSWT facility, which have a 30° pitch, 90° skew angle, and 1 mm diameter. The flat plate jet is scaled approximately 25x to a diameter of 25.4 mm. The pitch angle is defined as the angle the jet makes with the blade (or plate) surface. The skew angle refers to the angle the jet (projected to the surface) makes with the freestream flow direction. While the pitch and skew angle are fixed, this study looks at the effects of blowing ratio on boundary layer interaction. The blowing ratio is the ratio of the jet velocity to the freestream velocity, assuming the ratio of densities is unity. The frequency is fixed at f = 0.5 Hz for this crossflow study. A previous study[9] of the free jet (no crossflow) was performed at various duty cycles (fixed jet velocity and frequency). The free jet showed the same starting and ending events regardless of duty cycle. One variation of duty cycle was studied in this experiment to verify this was also true with the jet in crossflow. Then the duty cycle was fixed at Δ = 50% and only the blowing ratio was varied. Measurements were taken at seven spanwise planes for each case.

Figure 1 shows the location of each measurement plane as well as the orientation of the axes. Note that the origin is the center of the jet at the surface of the plate. Measurement planes of y = -1d, 0d, 1d, 2.25d, 3d, 4d, and 5.25d were studied. Figure 1 also indicates the placement of a ramp. The ramp is 22 mm tall at its peak and is used to force a separation region downstream of the ramp. The resulting separation region is about 25 mm tall, or one jet diameter.

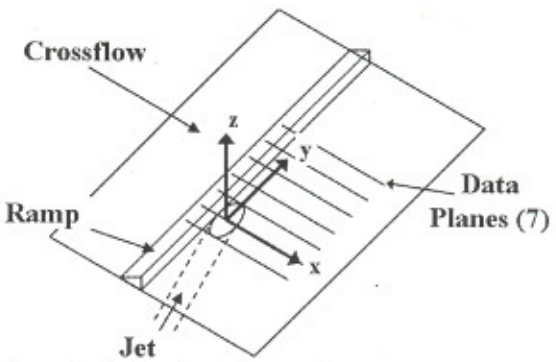

Figure 1. Axis orientation and measurement planes

II. Experimental Setup and Procedure

A. Setup

Figure 2 shows a schematic of the experimental setup. In this figure, the camera and laser light sheet are oriented to measure the free jet. In the current study, with the jet in crossflow, the camera and laser light sheet are rotated 90° clockwise to measure streamwise planes. The jet has length-to-diameter ratio of 12. The air for the jet comes through a 102 mm diameter plenum (406 mm long) and is fed through the bottom. Before it gets to the plenum, the

air passes through four high-speed Parker Instrumentation general valves (opening time less than 1 ms) connected in parallel, and controlled by a Parker Instrumentation Iota One pulse driver. The four valves in parallel give more of a range in jet velocity than using a single valve.

In order to seed the jet flow for the PIV measurements, a 0.1 m^3 plastic storage bin was used as a smoke box. Two 25 mm diameter tubes connected the smoke box to the feed plenum. One of these tubes allowed smoke into the plenum, and the other acted as a return so there would be no net mass flow into the plenum. The nozzle of the smoke machine (Safex F2010) was inserted into the smoke box to deliver the smoke. All connections to the smoke box were sealed with silicone RTV to ensure no losses in mass flow.

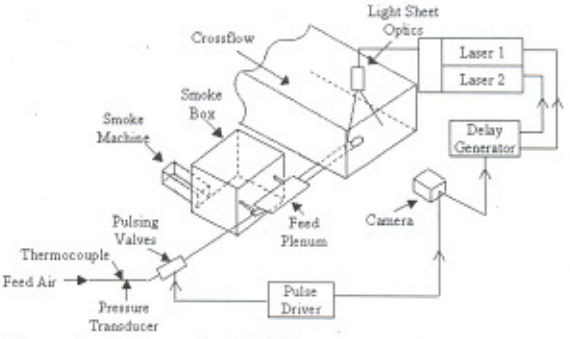

Figure 2. Schematic of PIV setup

The flat plate jet is mounted at the end of the Boundary Layer Tunnel of the AFRL. This tunnel allowed the development of a crossflow for this experiment. The tunnel has a 38.1 cm x 24.1 cm cross section. There is a settling chamber upstream of tunnel that contains turbulence reducing screens and honeycomb. The nozzle of a Rosco 4500 smoke machine was inserted into the side of the settling chamber to seed the crossflow. At 122 cm downstream of the exit of the settling chamber, there is a slot to bleed off the boundary layer. The center of the jet is located 2.53 m (99.6d) downstream of this bleed slot, and the boundary layer thickness at the jet location (without the ramp being present) is 70 mm (2.75d). A valve upstream of the settling chamber controls the crossflow velocity, and an upstream heat exchanger is used to control the temperature. The velocity of the crossflow was measured with a hot wire placed at x = 0d, y = 5.25d, and z = 3.31d, and was kept at 3.15 m/s. The temperature was typically 65°F (measured downstream of the heat exchanger and upstream of the settling chamber). The smoke machine was kept on during experimentation. The added mass flow was negligible and did not change the measured velocity of the crossflow.

The seeding was illuminated by a New Wave Pegasus-PIV dual head laser, each head capable of operating at up to 10 kHz. The rated energy at 1000 Hz is 10 mJ per pulse. The laser enclosure includes beam combining optics that output the beams from both laser heads through a single port. A Dantec light arm was used to guide the laser beam to the test section. A Dantec optics module was used to form the laser beam into a light sheet with a 20° spread angle and adjustable thickness. In this experiment, the sheet thickness was approximately 0.5 mm in the measurement plane.

Images of the flow field were captured by an IDT X-Stream VISION high-speed CMOS digital camera, capable of capturing images at up to 16 kHz in double frame mode at a resolution of 1260 x 40 pixels, and a 16 bit depth. Higher resolution (up to 1260 x 1024 pixels) can be obtained by operating the camera at slower capturing rates. The camera also has 4 gigabytes of on-board memory to temporarily store captured images until being saved to disk. For this setup, a resolution of 1260 x 752 pixels was used. This resolution provided a typical field of view 143 mm (5.63d) wide and 86 mm (3.39d) tall. A maximum number of 1300 image pairs could be captured at that resolution and stored in memory. Data was sampled at 50 Hz in order to obtain 13 cycles of data (100 image pairs per cycle, with the jet pulsing at 0.5 Hz) for ensemble averaging.

The camera triggers the laser through a delay generator, which triggers the first laser head in sync with the camera's first frame, and delays the second trigger (typically 200 μs) to provide the time differential between images. The camera was set to trigger off of the pulse driver, so that the image capture was phased locked with the valves.

B. Procedure

In this study, different blowing ratios ($B = \rho_j V_j / \rho_\infty U_\infty$) are tested. Since the jet air density, ρ_j, and the freestream air density, ρ_∞, are approximately equal ($\rho_j / \rho_\infty \approx 1$), the blowing ratio can be considered the ratio of the jet velocity, V_j, to the freestream velocity U_∞. The freestream velocity was fixed at U_∞ = 3.15 m/s, and the blowing ratios studied were B = 0, 0.5, 1, 2, and 4. The frequency was fixed at f = 0.5 Hz. At 0.5 Hz, the reduced frequency parameter ($F^+ = f\, l\, /\, U_\infty$) is matched to that of the experiments done in the LSWT (F^+ = 0.004, see Ref. 5) if one considers the reference length l to be the diameter of the jet. This would make l = 0.0254 m, f = 0.5 Hz, and U_∞ = 3.15 m/s, so F^+ = 0.004. Note that in Ref. 5 the reference length is the chord of the blade, but since the flat plate has no "chord", using the jet diameter as a reference length allows for a direct comparison of reduced frequency values. Also, the duty cycle was fixed at Δ = 50%. For a frequency of 0.5 Hz, this means that the valves that control the jet flow are open for one second of each two second cycle.

Images were captured using IDT X-VISION software, version 1.09.02, and were correlated with Dantec FlowManager version 4.30.27. Images were captured in 8-bit mode to save on disk space, and also because the 16-bit depth showed no difference in the quality of the captured images nor in the resulting correlations of the captured images. An adaptive correlation algorithm was used, where the images would be first correlated with 128 x 128 pixel interrogation regions, followed by a correlation of 64 x 64 pixel interrogation regions, and then by 32 x 32 pixel and finally 16 x 16 pixel interrogation regions. Each correlation step was repeated three times except for the final step, which was repeated four times. In each correlation pass, a 50% overlap was used, resulting in a final effective interrogation region size of 8 x 8 pixels. This provided an effective spatial resolution of 0.9 mm. Each correlation pass was also accompanied by a peak validation and a local median validation to help remove noise and outlying (erroneous) vectors. When the images were correlated, a moving average validation was performed on each of the resulting vector maps to remove any remaining outliers. Finally, an average filter was applied to further smooth out the vector field.

For all cases, the data was ensemble averaged using a MatLab routine that read in the correlated velocity data and output a TecPlot readable data file that also included a calculation of the vorticity field. TecPlot was then used to create animations of the velocity and vorticity plots. This allowed a look at each data plane individually. Another MatLab routine would be used to collect the data from each plane and create a single TecPlot readable file that contained all seven planes of data. Then three dimensional plots were created in TecPlot for each case. While both velocity and vorticity plots were obtained, only 3-D velocity plots will be presented here as they are sufficient to describe the flow characteristics.

III. Results

A. Uncertainty and Verification of PIV Data

In order to get an idea of the variability in the PIV results, one case (f = 4 Hz, Δ = 50%, B = 1) of the free jet (no crossflow) was run six times. Each of the six cases was ensemble averaged over 13 cycles of data. The average velocity over the entire cycle over the expanse of the jet exit (averaging in space and time) was compared for each of the six cases. The mean velocity was 0.78 m/s, with a standard deviation of 0.022 m/s. The percent error could be thus estimated as 2.8%. There is also a measurement error to consider, combining bias and RMS errors, which is typically about 0.1 pixels.[10] In the current setup, 0.1 pixels is equivalent to 0.035 m/s. As a percentage of the mean velocity of 0.78 m/s, this error is 4.5%. The root sum of squares of these two errors is 5.3%.

B. Duty Cycle Comparison

With the free jet in the previous study[9], the focus was the effect of duty cycle. There were no noteworthy differences between the starting and ending dynamics of the pulses for the different duty cycles. To see if the same were true for the jet in crossflow experiment, one case was run at Δ = 10% and then at Δ = 50%. The plane was y = 5.25d, with the jet pulsing at f = 0.5 Hz (F^+ = 0.004) and blowing at B = 2.

The jet is open for the first 10% of the Δ = 10% case. This first part of the Δ = 10% case is shown in the velocity and vorticity plots of Fig. 3a (t = 0.02, 0.06, 0.08, and 0.10). Likewise, the first 10% of the Δ = 50% case is shown in Fig. 3b. In these figures, the velocity has been normalized by U_∞, and the vorticity by U_∞/d. The black area in each figure represents the location of the ramp. One can see by comparing the figures that the first part of the cycle is virtually identical for both cases. The 10% part of the cycle after the valve closes for both cases is shown in Fig. 4. This time interval is t = 0.10 – 0.20 for Δ = 10% (with t = 0.12, 0.14, 0.16, and 0.20 shown in Fig. 4a) and t = 0.50 – 0.60 for Δ = 50% (with t = 0.52, 0.54, 0.56, and 0.60 shown in Fig. 4b). Again the data from these time intervals appear very similar for the two cases. Therefore, the effect of the jet on the crossflow is not strongly dependent on duty cycle for this frequency. The primary difference is that the effect of the higher duty cycles lasts longer, because the jet is on longer. At a higher frequency this may not be the case because the jet would not be on as long.

C. B = 4 Case

Since changing the duty cycle does not affect the crossflow dynamics, but merely the length of time the crossflow spends in "steady state", the primary parameter of interest is the blowing ratio. As mentioned previously, blowing ratios of B = 0.5, 1.0, 2.0, and 4.0 were studied. Each case was fixed at a frequency of f = 0.5 Hz and a duty cycle of Δ = 50%. All seven of the two dimensional planes were combined into one three dimensional animated plot for each case, with 20 ms between each frame due to the 50 Hz sampling rate. Select frames from each of these animated plots will be shown.

Figure 5a shows the initial fully separated state of the flow for the B = 4 case at time $t = 0.00$. The location of the jet is drawn onto the figure for reference. The ramp is not shown, but it is just upstream of the jet and extends across the entire span. Notice the reverse flow and circulation in the separated region. At this moment, the valves open and the air begins flowing to the jet. At $t = 0.01$ (Fig. 5b) the jet flow has entered the y = 0d plane. Behind the jet flow, in the y = -1d plane, is a downward motion of air flow due to the entrainment caused by the starting vortex. This initial downward motion near the jet is maintained as the jet continues to entrain the air around it. As the jet flow penetrates deeper into the freestream, this entrainment causes the crossflow to swirl around the core of the jet flow. The jet flow does not mix well with the crossflow in this case because the jet flow momentum is so much higher and is not affected much by the crossflow. This can be seen at $t = 0.05$ (Fig. 5c), as the jet has penetrated through the y = 5.25d plane. The air downstream of the jet flow is drawn downward in the y = -1d and 0d planes, but is then drawn upward in the y = 2.25d, 3d, 4d, and 5.25d planes. There is likely much out of plane motion (which is not measured) in the y = 1d plane as the jet flow is drawing this downstream air towards itself. The flow has reached a "steady" state by $t = 0.20$ (Fig. 5d), with the flow attached in the y = -1d, 0d, and 1d planes, a large amount of reverse flow in the y = 2.25d and 3d planes, and more attachment in the y = 4d and 5.25d planes. In the y ≥ 2.25d planes, any flow downstream of the jet flow is drawn back upstream towards the jet. This is the freestream swirling around the jet flow. At $t = 0.5$ (Fig. 5e), the valves close and stop the air flow to the jet. Without the momentum sustaining the jet flow, the crossflow begins to take over. This can be seen at $t = 0.55$ (Fig. 5f), where the previously obstructed crossflow (in the planes y ≥ 2.25d) is now able to flow in the downstream direction. In the y = 2.25d plane, the drastic change in momentum causes a circulation region that draws freestream air downward as the shear layer reestablishes. By $t = 0.57$ (Fig. 5g), the flow is attached across the entire measured span (y = -1d to y = 5.25d). The shear layer stabilizes and the flow returns to its fully separated state by $t = 0.67$, with the last bit of attachment seen at $t = 0.66$ (Fig. 5h).

Although not shown here, the vorticity plots indicate a maximum in-plane vorticity (normalized by U_∞/d) of ω_j = 8.05 and a minimum of ω_j = -5.83 for this case. Note that only the spanwise component of vorticity can only be calculated because velocity data is only available in the x-z plane. The maximum vorticity occurs at x = -0.72d, z = 0.98d in the y = 4d plane, and at $t = 0.34$. This point is very close to the ramp tip, which is located at x = -0.87d, z = 0.87d, indicating the large amount of vorticity is in the shear layer. The minimum vorticity occurs at x = 4.03d, z = 0.31d, in the y = 3d plane, and at $t = 0.10$.

D. $B = 2$ Case

The $B = 2$ case starts out the same as the $B = 4$ case, with fully separated flow at $t = 0.00$. In this case the jet flow is just barely seen at $t = 0.01$, and more apparent at $t = 0.02$ (Fig. 6a). A similar effect is seen at the start of the cycle with the initial downward movement of air just upstream of the jet (in the y = -1d plane) as the starting vortex entrains the air around the jet flow. In this case the jet flow is not as strong and does not entrain the air around it as it did in the $B = 4$ case. This can be seen at $t = 0.09$ (Fig. 6b), as the jet has penetrated through the y = 3d plane, and is having an impact on the y = 4d plane as it gets turned downstream. The jet flow in the $B = 2$ case has much lower momentum than the $B = 4$ case, and the jet flow does not maintain its form long as it penetrates into the crossflow. However, there is some entrainment in the y = 1d and 2.25d planes as the jet flow draws downstream air towards itself. There is also attachment in the y = 5.25d plane. As the flow reaches a steady state ($t = 0.20$, Fig. 6c), the flow in the y = 4d plane becomes attached as well. The attachment in the y = 4d and 5.25d planes is present in this case and not in the $B = 4$ case because the jet flow has turned downstream instead of acting as an obstruction to the crossflow. After the jet turns off (i.e. the valves close), the flow behavior is similar to the $B = 4$ case. By $t = 0.55$ (Fig. 6d), the crossflow has started to take over, most notably at y = 2.25d as in the $B = 4$ case, where a circulation region has formed bringing freestream air down to the surface. As in the $B = 4$ case, there is spanwise attachment at $t = 0.57$ (Fig. 6e), but here the last attachment comes at $t = 0.62$ (Fig. 6f) before the flow returns to its fully separated state. The maximum vorticity in this case is ω_j = 7.89, and occurs at x = -0.76d, z = 1.02d, in the y = 4d plane, and at $t = 0.28$. Note that there is not much of a change from the previous case to this case in maximum vorticity. The minimum vorticity in this case is ω_j = -3.52, and occurs at x = 1.08d, z = 0.74d, in the y = 3d plane, and at $t = 0.06$.

E. $B = 1$ Case

The $B = 1$ jet flow is apparent at $t = 0.02$, but is better seen at $t = 0.03$ (Fig. 7a). In this case the downward motion in the y = -1d plane is barely noticeable. The momentum of the jet flow is so much lower in this case that the jet flow gets turned downstream almost immediately upon penetrating the crossflow in the y = 2.25d plane. Figure 7b shows the "steady" state flow at $t = 0.20$, with the trailing edges of the y = -1d and y = 3d planes going in and out of attachment. The y = 4d plane shows nearly full attachment. The y = 5.25d plane is an indicator of how weak the $B = 1$ jet really is, as it has almost no effect that far away. The y = 1d plane shows some entrainment of downstream

air as the jet flow is still strong enough to draw that air towards itself. The $B = 2$ and $B = 4$ cases showed a circulation region form at y = 2.25d after the jet turned off. In this $B = 1$ case, this same effect occurs but at y = 1d and at $t = 0.53$ (Fig. 7c). This brings near attachment in the y = -1d through y = 4d planes at $t = 0.55$ (Fig. 7d). However, this weak attachment only persists until $t = 0.56$, except in the y = 2.25d plane, where it lasts until $t = 0.59$. The flow then is fully separated. The maximum vorticity for the $B = 1$ case is $\omega_j = 5.79$, and occurs at x = -0.94d, z = 0.96d, in the y = 3d plane, and at $t = 0.18$. The minimum vorticity is $\omega_j = -2.03$, at x = -0.15d, z = 1.64d, y = 0d, and $t = 0.71$.

F. $B = 0.5$ Case

In the $B = 0.5$ case, the jet flow is too weak to even penetrate into the crossflow. It therefore has no noticeable effect on the crossflow. The beginning, end, and steady part of the cycle all appear the same as the fully separated flow in Fig. 7. The maximum vorticity in this case is $\omega_j = 4.96$, and occurs at x = -1.10d, z = 1.01d, in the y = -1d plane, at $t = 0.33$. The minimum vorticity is $\omega_j = -1.88$, at x = 3.12d, z = 0.29d, y = 5.25d, and $t = 0.01$.

G. $B = 0$ Case

There was no actual $B = 0$ case run. Rather, the data from the $B = 0.5$ case at $t = 0.00$ was used to approximate the case of no jet blowing ($B = 0$). This is a reasonable approximation because of how small the effect of the $B = 0.5$ jet was, and because whatever effect there may have been would not be evident at $t = 0.00$. Using this data, the maximum vorticity in the $B = 0$ case is $\omega_j = 4.83$, and occurs at x = -0.63d, z = 1.04d, and in the y = -1d plane. The minimum vorticity is $\omega_j = -1.52$, at x = 4.09d, z = 0.07d, and y = 5.25d.

A summary of the maximum and minimum vorticity is given in Fig. 8. The trend is increasing vorticity (both positive and negative) for increasing blowing ratios, although the maximum vorticity appears to be leveling off at the higher B values.

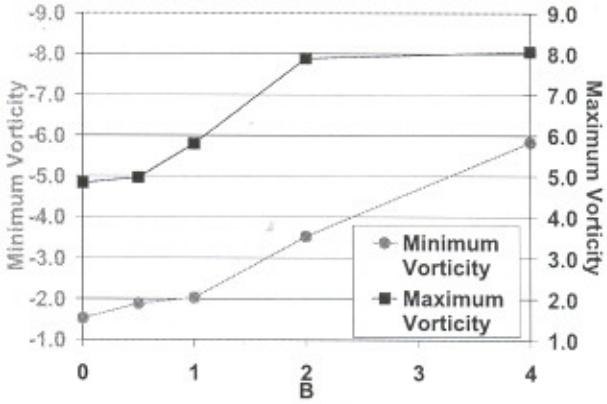

Figure 8. Maximum and Minimum Vorticity

IV. Conclusions

After determining that differences in duty cycles were not significant enough to perform a duty cycle study as done previously, this experiment focused on the changes in blowing ratio, which was varied from $B = 0$ to $B = 4$. Seven spanwise planes were studied, spaced nominally in 1d increments and centered in the tunnel. The frequency was 0.5 Hz, and the duty cycle was 50% for all cases. Perpendicular (cross-stream) planes were attempted, but the out of plane motion was too great to obtain good PIV results. Damping in the system (the smoke box and plenum being the main contributors) caused a low-frequency limitation, and the jet could not be pulsed fast enough to maintain an attached flow for much longer than the duty cycle. Attachment was seen for blowing ratios as low as unity, although greater blowing ratios resulted in more attached area and longer attached times. It was determined that not only the starting event but also the ending event of the cycle were keys in eliminating separation. The starting event because it provided that first impulse that pulls the crossflow towards the surface, and the ending event because it provided sudden change in momentum that brought spanwise attachment for the $B = 2$ and $B = 4$ cases. The improvement in attachment with increasing blowing ratio was also accompanied by an increase in vorticity. The maximum vorticity in each case occurred in near the ramp tip, or near the beginning of the shear layer, and always occurred when the jet was in a "steady" state (i.e. not near the beginning and ending transitions). During the actual flow of the jet, attachment was not spanwise in these cases. In fact only three of the seven planes in the $B = 2$ and $B = 4$ cases showed any attachment during the duty cycle. The $B = 1$ case only showed attachment in two planes. This showed the need for optimizing spacing of the jets to provide spanwise attachment. Spanwise attachment could also occur if the pulsing frequency was optimized, so the effect of the beginning and ending events can be used to keep the flow attached for longer periods of time. The optimization of frequency, duty cycle, blowing ratio, and spanwise spacing of the jets will help to reduce the required mass flow for obtaining an attached boundary layer using pulsed vortex generator jets.

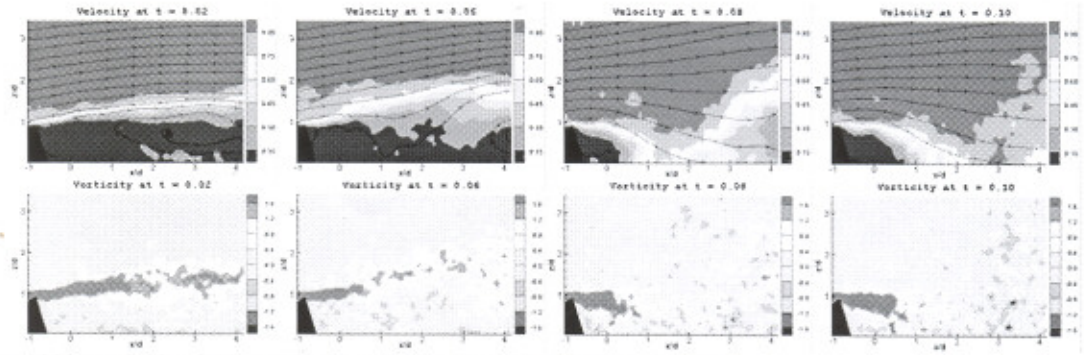

a) $\Delta = 10\%$, $t = 0.00 - 0.10$ (select instances at the beginning of the cycle)

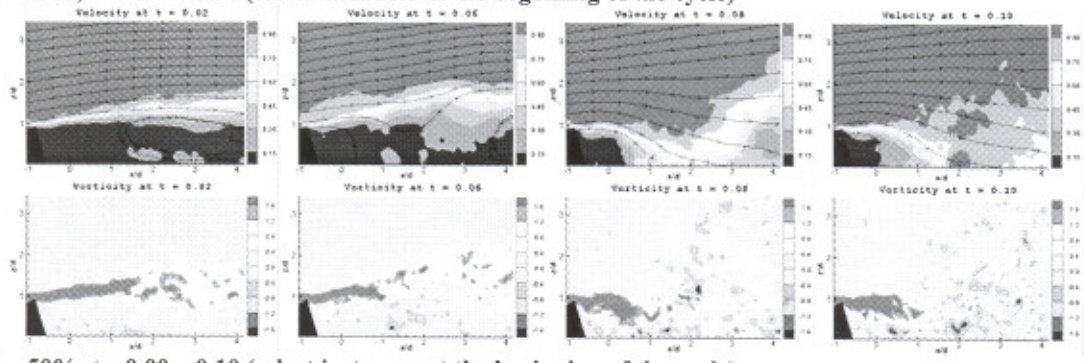

b) $\Delta = 50\%$, $t = 0.00 - 0.10$ (select instances at the beginning of the cycle)

Figure 3. First 10% of the $\Delta = 10\%$ case (a) and $\Delta = 50\%$ case (b), $F^+ = 0.004$, $B = 2$, y = 5.25d. The plots are velocity magnitude normalized by U_∞ (top), and in-plane vorticity normalized by U_∞/d (bottom).

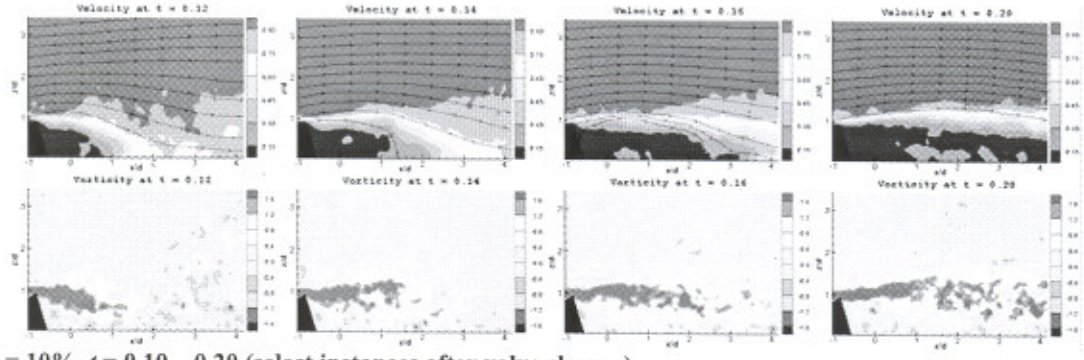

a) $\Delta = 10\%$, $t = 0.10 - 0.20$ (select instances after valve closure)

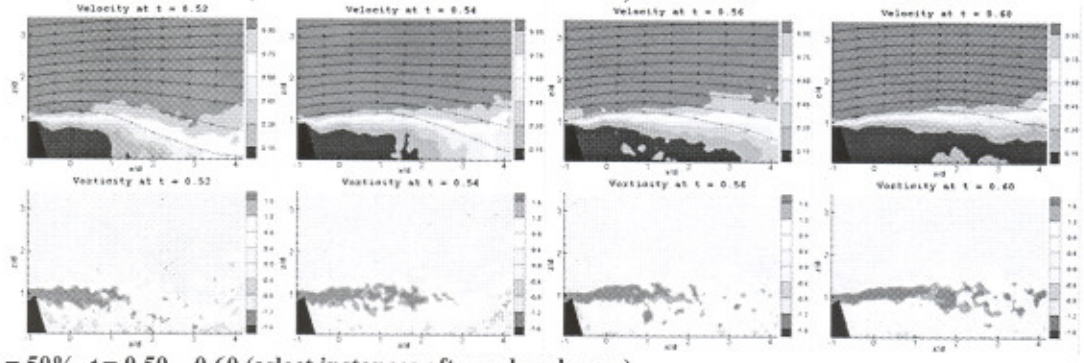

b) $\Delta = 50\%$, $t = 0.50 - 0.60$ (select instances after valve closure)

Figure 4. First 10% after valve closure of the $\Delta = 10\%$ case (a) and $\Delta = 50\%$ case (b), $F^+ = 0.004$, $B = 2$, y = 5.25d. The plots are normalized as in Fig. 3.

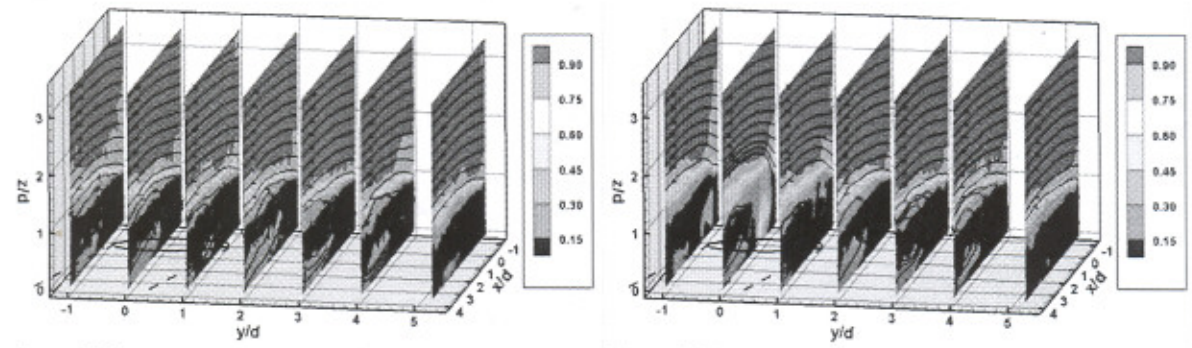

a) $t = 0.00$ b) $t = 0.01$

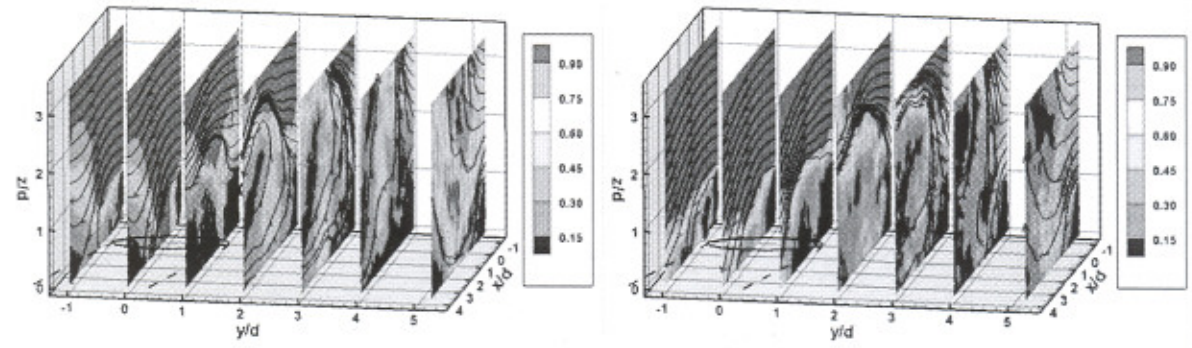

c) $t = 0.05$ d) $t = 0.20$

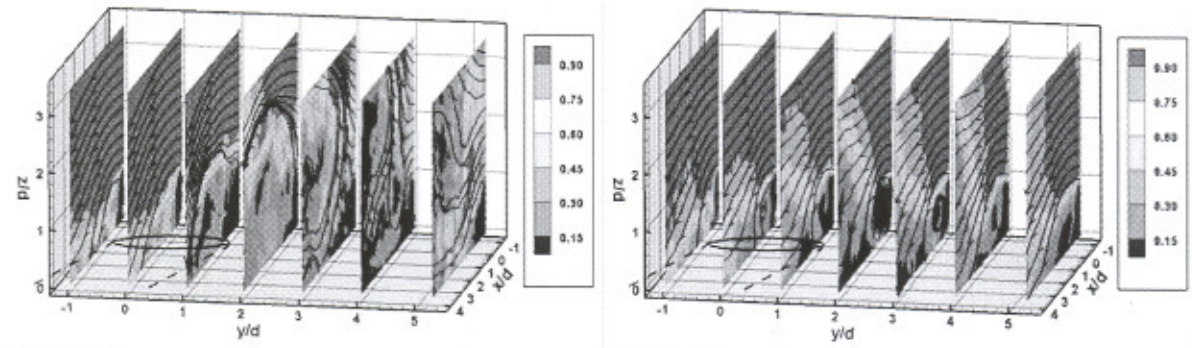

e) $t = 0.50$ f) $t = 0.55$

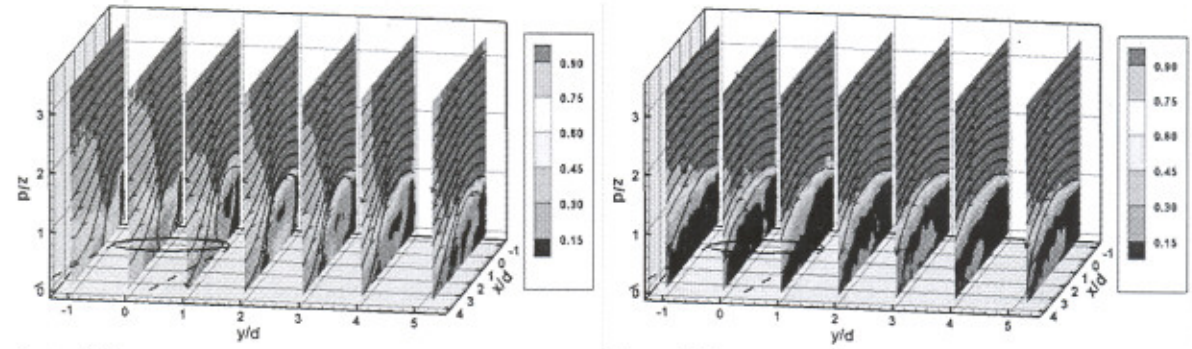

g) $t = 0.57$. h) $t = 0.66$

Figure 5. Normalized velocity plots (velocity magnitude divided by U_∞) for $B = 4$, $F^+ = 0.004$Hz, $\Delta = 50\%$ case

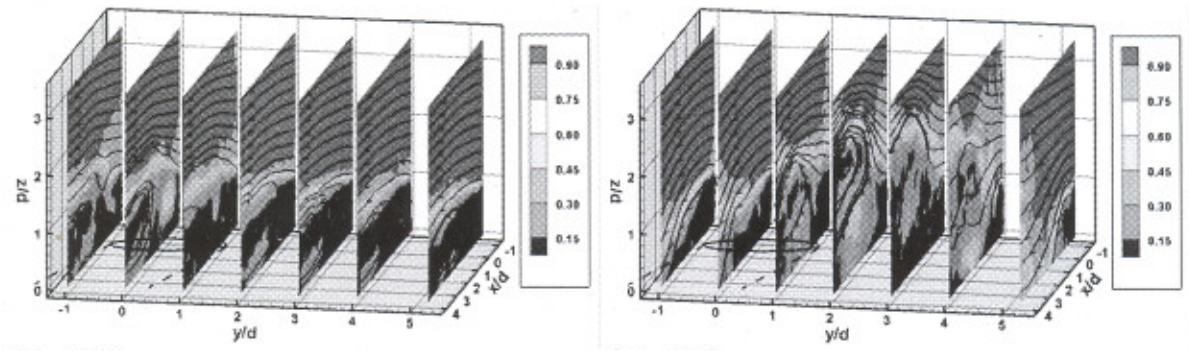

a) $t = 0.02$ b) $t = 0.09$

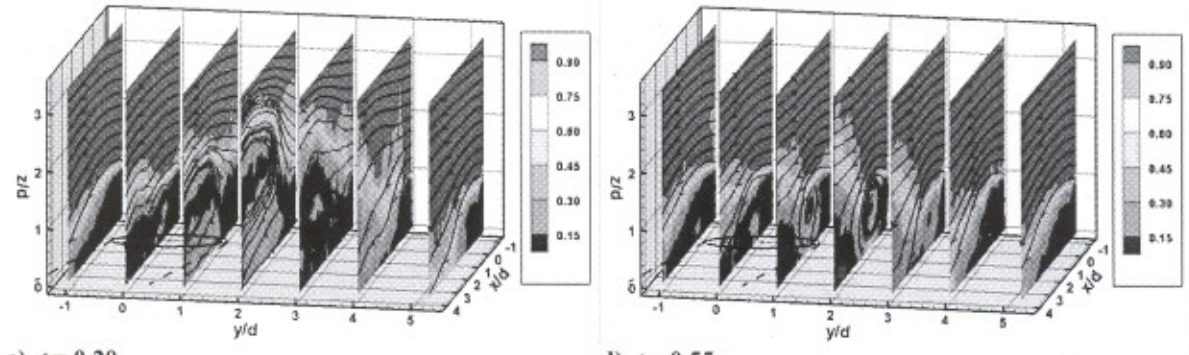

c) $t = 0.20$ d) $t = 0.55$

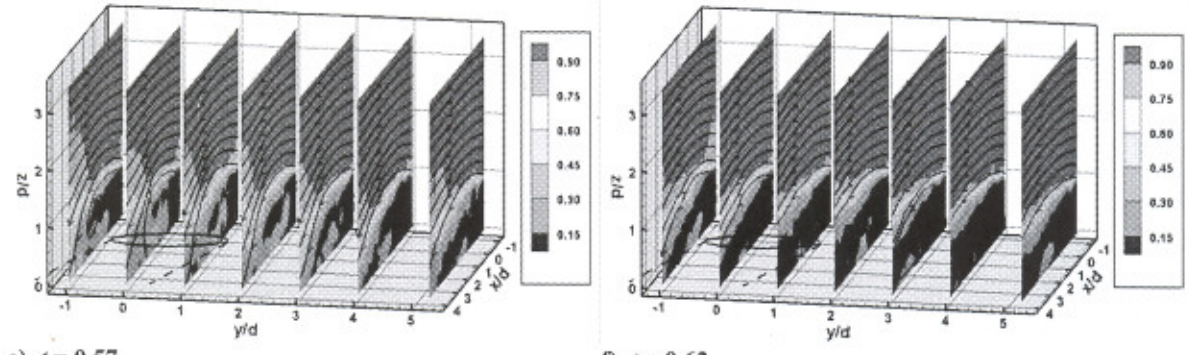

e) $t = 0.57$ f) $t = 0.62$

Figure 6. Normalized velocity plots (velocity magnitude divided by U_∞) for $B = 2$, $F^+ = 0.004$, $\Delta = 50\%$ case

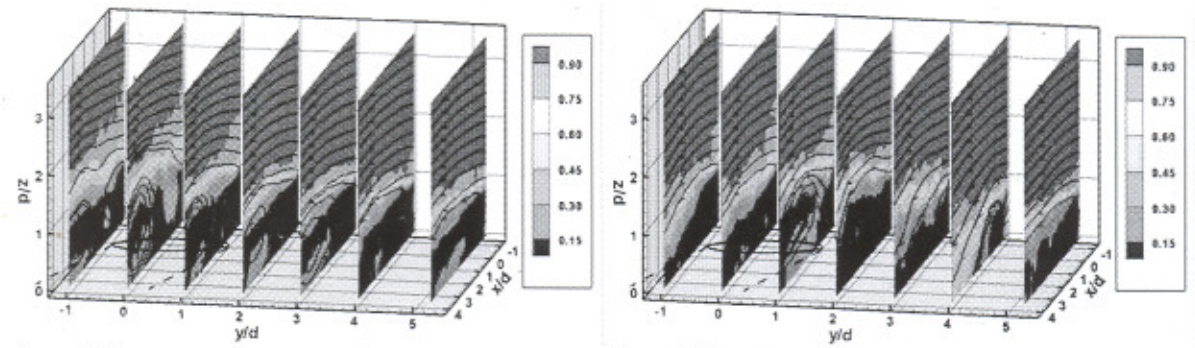

a) $t = 0.03$ b) $t = 0.20$

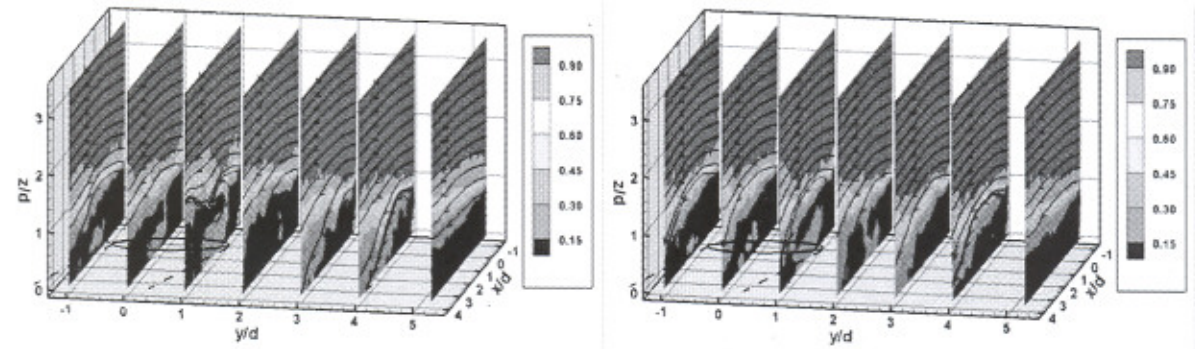

c) $t = 0.53$ d) $t = 0.55$

Figure 7. Normalized velocity plots (velocity magnitude divided by U_∞) for $B = 1$, $F^+ = 0.004$, $\Delta = 50\%$ case

V. Acknowledgments

The authors would like to thank the Dayton Area Graduate Studies Institute (DAGSI), contract PR-UC-01-07, and the Air Force Research Laboratory (AFRL), contract F33615-98-C-2895, for their financial support for this research, and the AFRL for the use of their facilities. The assistance of Dr. Chuck Cross, Gary Terborg, Dr. Greg Minkiewicz, Dr. Campbell Carter, Dr. Richard Rivir, and others in the Propulsion Directorate of AFRL is also acknowledged.

VI. References

[1]Lake J P., "Flow Separation Prevention on a Turbine Blade in Cascade at Low Reynolds Number," Ph.D. Dissertation, Air Force Institute of Technology, Dayton, OH, 1999.

[2]Rivir R, White A, Carter C, and Ganguly B., "AC and Pulsed Plasma Flow Control," AIAA 2004-847, 2004.

[3]List J, Byerley A, McLaughlin T, and Van Dyken R., "Using a Plasma Actuator to Control Laminar Separation on a Linear Cascade Turbine Blade," AIAA 2003-1026.

[4]Bons J, Sondergaard R, and Rivir R., "Turbine Separation Control Using Pulsed Vortex Generator Jets," *ASME Journal of Turbomachinery*, Vol. 123, No. 4, 2001, pp. 198-206.

[5]Bons J, Sondergaard R, and Rivir R., "The Fluid Dynamics of LPT Blade Separation Control Using Pulsed Jets," *ASME Journal of Turbomachinery*, Vol. 124, No. 1, 2002, pp. 77-85.

[6]Johari, H. and McManus, K.R., "Visualization of Pulsed Vortex Generator Jets for Active Control of Boundary Layer Separation," AIAA 97-2021, 1997.

[7]Compton, D.A. and Johnston, J.P., "Streamwise Vortex Production by Pitched and Skewed Jets in a Turbulent Boundary Layer," *AIAA Journal*, Vol. 30, No. 3, 1992, pp. 640-647.

[8]McManus, K., Ducharme, A., Goldey, C., and Magill, J., "Pulsed Jet Actuators for Suppressing Flow Separation," AIAA 96-0442, 1996.

[9]Moore, K., Wolff, M., Polanka, M., and Sondergaard, R., "A PIV Study of Pulsed Vortex Generator Jets," AIAA 2004-3927, 2004.

[10]Huang H, Dabiri D, and Gharib M., "On Errors of Digital Particle Image Velocimetry," *Measurement Science and Technology*, Vol. 8, No. 12, 1997, pp. 1427-1440.